Johann Radon Institute for
Computational and Applied Mathematics
Austrian Academy of Sciences (ÖAW)

The Finite Line Integration Method (FLIM) - A Fast Variant of Finite Element Modelling

J. Synka

RICAM-Report 2007-27

The Finite Line Integration Method (FLIM) - A Fast Variant of Finite Element Modelling

Josef SYNKA

Industrial Mathematics Institute, Johannes Kepler University,
Altenberger Str. 69, A-4040 Linz, Austria (josef.synka@jku.at)

Abstract

A new way of modelling and solving partial differential equations is derived. While the finite element (FE) methodology is based on the integration over finite elements, this novel approach utilizes edges (finite lines) instead, which results in a finite line integration (FLIM). We present how the FE-computations over elements (areas or volumes) can be rewritten for the stiffness matrix based on edges and how the load can be obtained along these finite lines. It is shown that the performance of the new method can be made identical to the performance of the finite element method (FEM) for linear triangular or tetrahedral elements independent of the mesh being structured or unstructured. The new method, however, requires much lower storage than FEM, especially for three-dimensional problems, but yields the same approximation error and convergence rate as the finite element method. Further, this approach allows for a direct computation of stiffness matrices at edge level, which can advantageously be used for the development of efficient linear iterative solvers.

AMS Subject Classifications: 65D30, 65N30.

Keywords: Finite element method, line integration, edge matrices, weak formulation, computational methods.

1 Introduction

Over the last decades, the finite element method has established itself as one of the most powerful ways of solving partial differential equations. The introduction of Sobolev spaces provided a strong framework for the theoretical study of existence and uniqueness results, which has resulted in a nearly countless number of contributions to literature (see, e.g., Braess [1], Zienkiewicz and Taylor [12], Brenner and Scott [2], Schwarz [10], Krizek [8], Johnson [5], or Ciarlet [3], to mention just a few).

Due to the popularity of FEM in engineering sciences and industrial applications, increasing effort has been made in improving its performance. One of the main foci lies on a robust and highly efficient solution of the resulting system of linear equations. It is obvious that the

more information on the problem can be inserted the faster the method for its solution will be. For the development of fast solvers based on Algebraic Multi-Grid (AMG) methods, it can thus be useful to base their construction on the information contained in edge rather than in element matrices. Another advantage of this approach lies in the fact that edge matrices require less storage compared to their element counterparts, which is particularly the case in three-dimensional problems. The potential advantages of an edge-based finite element formulation are also mentioned by Zienkiewicz et al. [13] (Appendix F) in the context of fluid dynamics. In two dimensions our formulation is related to the approach of Hackbusch [4]. However, the finite line integration method does not require the concept of box schemes and is also applicable in three dimensions.

At present, we will restrict ourselves to triangular and tetrahedral meshes. We will show that in both, two and three, dimensions the computation of the global stiffness matrix via elements or edges yields an identical matrix. The difference between these two approaches lies in the treatment of the load. While in FEM the load is calculated over finite elements (areas in 2D and volumes in 3D), the new method - referred to as FLIM (Finite Line Integration Method) - determines the load only along the edges of the elements. In the present study we will thereby assume that the triangles or tetrahedra are bounded by straight lines. It will be shown that the new approach allows for a direct (integration-free) calculation of the edge stiffness matrices; numerical integration is only required for the computation of the load contributions along a element boundaries (edges).

Numerical computations reveal that for constant sources FLIM yields a system of linear equations which is identical to the one obtained with FE-modelling based on linear triangles (in 2D) or linear tetrahedra (in 3D) in any case. Based on proper quadrature rules for the approximation of the sufficiently smooth linear functional on the right-hand side, as required by FEM, it can further be shown that the new method with a properly chosen approximation of the load can be rendered equivalent to FEM concerning the approximation and convergence properties, but is much cheaper concerning storage and setup of the global stiffness matrix.

The paper is organized as follows: In Section 2 we present the concept of the (finite) line integration method, such as the computation of the edge stiffness matrices and the edge load vector. In Section 3 we discuss how the approximation error and convergence rate of FLIM can be related to their FEM-counterparts by choosing proper quadrature schemes for the line integration method and derive such schemes. We further show that the storage requirements for the assembling process are significantly reduced when using FLIM and we remark on possible advantages of using edge matrices for the establishment of new AMG-based iterative solvers. The numerical results on two-dimensional problems with different right-hand sides (sources), as presented in Section 4, support the theoretical observations and confirm the strengths of the new edge-based variant of FEM, when compared to the outcomes of standard element-based FEM computations. The paper is concluded with a summary of the main features of the new modelling technique in Section 5.

2 The Concept of Finite Line Integration versus FEM

2.1 Weak formulation and summation over finite elements

In our study we consider boundary value problems of the form

$$\begin{aligned} -\mathrm{div}\,[c(\mathbf{x})\,\mathrm{grad}\,u(\mathbf{x})] &= f(\mathbf{x}) \qquad \text{in} \quad \Omega\ (\subset \mathbb{R}^d)\ \text{with}\ d \in \{2,3\} \\ u(\mathbf{x}) &= 0 \qquad\quad \text{on} \quad \Gamma := \partial\Omega\,, \end{aligned} \tag{1}$$

for which the weak formulation reads (in index notation with $i = 1, \ldots, d$) as

$$\int_\Omega c_{km}(\mathbf{x})\,\nabla_m\,u(\mathbf{x})\,\nabla_k\,w(\mathbf{x})\,d\mathbf{x} = \int_\Omega f(\mathbf{x})\,w(\mathbf{x})\,d\mathbf{x}\,. \tag{2}$$

Thereby, ∇_k denotes the partial derivative w.r.t. x_k, w designates a weighting function, u is the unknown function, and $u,\ w \in H_0^1(\Omega) := \{v \in H^1(\Omega) : v = 0 \text{ on } \Gamma\}$. The matrix $c(\mathbf{x}) := (c_{km}(\mathbf{x}))_{\,k,m\in\{1,2,\ldots,d\}}$ is assumed to be bounded, symmetric and uniformly positive definite in Ω with piecewise smooth functions $c_{km}(\mathbf{x})$ in $\bar{\Omega} := \Omega \cup \partial\Omega$. Throughout this paper, we will make use of Einstein's summation convention, i.e., a repeated index in a term will be summed over its index set (unless indicated otherwise), and of the standard assumptions on triangulation.

Let n_e denote the total number of finite elements Ω_e in the partition of $\bar{\Omega}$. Then, (2) can be rewritten in the form

$$\sum_{e=1}^{n_e} \int_{\Omega_e} c_{km}(\mathbf{x})\,\nabla_m\,u(\mathbf{x})\,\nabla_k\,w(\mathbf{x})\,d\mathbf{x} = \sum_{e=1}^{n_e} \int_{\Omega_e} f(\mathbf{x})\,w(\mathbf{x})\,d\mathbf{x}\,. \tag{3}$$

Note that the concept introduced herein can easily be extended to more complex problems involving mass and/or other types of boundary constraints. It should further be noted that the weak formulation, given in (3), also forms the basis for the finite line integration method, but with the integrals over finite triangular elements then being replaced by integrals along the edges of these triangular elements (see Section 2.3).

2.2 Fast computation of element matrices for FEM

It is well-known in the finite element theory that for triangles and tetrahedra bounded by line segments the usage of so-called base element matrices allow for a fast computation of the element stiffness matrices (cf. Schwarz [10]), which we will outline in this section. In Section 2.3 we will then extend this concept to obtain a fast computation method for base edge matrices and we will show that, when assembled, the base edge matrices corresponding to a particular finite element yield exactly the same element stiffness matrix as obtained via the finite element approach. All the element matrices can then be assembled in the usual way to form an identical global stiffness matrix in FEM and FLIM.

Let us first consider the fast computation of element matrices in FEM. The left-hand side of Eq. (3) for an arbitrary but fixed finite element Ω_e can be transformed to the local coordinate system by the chain rule of calculus, which yields

$$\int_{\Omega_e} c_{km}(\mathbf{x})\,\nabla_m u(\mathbf{x})\,\nabla_k w(\mathbf{x})\,d\mathbf{x} \;=\; \int_{\Omega_e^{\mathrm{loc}}} \bar{w}^{(i)}\,J\,\xi_{p,m}\,\xi_{q,k}\;\hat{c}_{km}(\boldsymbol{\xi})\,\Phi_{i,p}(\boldsymbol{\xi})\,\Phi_{j,q}(\boldsymbol{\xi})\,\bar{u}^{(j)}\,d\boldsymbol{\xi}\,, \qquad (4)$$

where $1 \le k,p,q,m \le d$ with d denoting the dimension of the problem, $1 \le i,j \le n_N^e$ with n_N^e being the total number of nodes of a finite element (i.e., $n_N^e = 3$ (4) for linear triangular (tetrahedral) elements), and $\hat{c}_{km}(\boldsymbol{\xi}) := c_{km}(\mathbf{x}(\boldsymbol{\xi}))$ is the (k,m)-th element of the matrix $c(\mathbf{x})$ in the local coordinate system $\boldsymbol{\xi}$. With $\xi_{p,k}$ we denote the derivative $\xi_{p,k} := \dfrac{\partial \xi_p}{\partial x_k}(\mathbf{x})$, which can be computed as $\xi_{p,k} = \left(\dfrac{\partial \mathbf{x}}{\partial \boldsymbol{\xi}}(\boldsymbol{\xi})\right)^{-1}_{pk}$ and the Jacobian is given by $J := \det\left(\dfrac{\partial \mathbf{x}}{\partial \boldsymbol{\xi}}(\boldsymbol{\xi})\right)$. Further, we utilize the setting $u(\boldsymbol{\xi}) := \Phi_i(\boldsymbol{\xi})\,\bar{u}^{(i)}$, where Φ_i denotes the i-th shape function for the approximation of u, while the corresponding nodal value of u is designated by $\bar{u}^{(i)}$. The same holds for the representation of the weighting function w, which based on a Galerkin approach is assumed to lie in the vector space of u.

In the present study we will restrict our discussion to linear geometry mapping, where the Jacobian J as well as the derivatives $\xi_{p,k}$ for a given p, k are constant. An extension of the presented concept to curvilinear elements is possible. For convenience, let us further assume that $c(\mathbf{x}) \equiv 1$, i.e., the identity in the following. Then, the expression $\xi_{p,m}\,\hat{c}_{km}(\boldsymbol{\xi})$ in (4) simplifies to $\xi_{p,k}$. An extension of the derivations given below to arbitrary settings of $c(\mathbf{x})$, however, is possible and straightforward.

Definition 2.1 *For arbitrary but fixed p, $q \in \{1,\ldots,d\}$ with d designating the dimension of the problem (viz., 2D or 3D), let the factors resulting from the transformation to local coordinates be defined as (summation over k)*

$$a_{pq} := J\,\xi_{p,k}\,\xi_{q,k}\,, \qquad (5)$$

and let the corresponding base element matrix S_{pq}^e be defined as (no summation)

$$S_{pq}^e := \left(\int_{\Omega_e^{\mathrm{loc}}} \Phi_{i,p}(\boldsymbol{\xi})\,\Phi_{j,q}(\boldsymbol{\xi})\,d\boldsymbol{\xi}\right)_{ij} \qquad (1 \le i,j \le n_N^e). \qquad (6)$$

With Defintion 2.1 in hand, we can now rewrite Eq. (4) in a decomposed form as

$$\int_{\Omega_e} \nabla_k u(\mathbf{x})\,\nabla_k w(\mathbf{x})\,d\mathbf{x} \;=\; \sum_{1\le p,q\le d} \bar{\mathbf{w}}\,a_{pq}\,S_{pq}^e\,\bar{\mathbf{u}}\,, \qquad (7)$$

where $\bar{\mathbf{u}}$ and $\bar{\mathbf{w}}$ respectively denote the vectors of the nodal values of u and of the coefficients of w of size n_N^e, which correspond to element e, and summation is to be taken over k.

Remark 2.1 *For triangles, bounded by line segments, the (symmetric) factors a_{pq} read as follows (cf. Schwarz [10], Section 2.2):*

$$\begin{aligned} a_{11} &= \|\mathbf{x}^{3-1}\|^2 / J \\ a_{12} &= -\langle \mathbf{x}^{3-1}, \mathbf{x}^{2-1} \rangle / J \\ a_{22} &= \|\mathbf{x}^{2-1}\|^2 / J \,, \end{aligned} \tag{8}$$

where $\mathbf{x}^{i-j} := \mathbf{x}^i - \mathbf{x}^j$ and $J := (x_{21} - x_{11})(x_{32} - x_{12}) - (x_{31} - x_{11})(x_{22} - x_{12})$. For the corresponding values for tetrahedral elements, see Theorem 2.1 and the proof thereof.

For a linear approximation of the unknown function u, the vector of shape functions and the related Jacobian matrix are respectively given for the triangle as

$$\Phi(\boldsymbol{\xi}) := \begin{pmatrix} 1 - \xi_1 - \xi_2 \\ \xi_1 \\ \xi_2 \end{pmatrix} \qquad \text{and} \qquad J_\Phi(\boldsymbol{\xi}) := \begin{pmatrix} -1 & -1 \\ 1 & 0 \\ 0 & 1 \end{pmatrix}, \tag{9}$$

and for the tetrahedron as

$$\Phi(\boldsymbol{\xi}) := \begin{pmatrix} 1 - \xi_1 - \xi_2 - \xi_3 \\ \xi_1 \\ \xi_2 \\ \xi_3 \end{pmatrix} \qquad \text{and} \qquad J_\Phi(\boldsymbol{\xi}) := \begin{pmatrix} -1 & -1 & -1 \\ 1 & 0 & 0 \\ 0 & 1 & 0 \\ 0 & 0 & 1 \end{pmatrix}. \tag{10}$$

Remark 2.2 *The base element matrices for triangular elements are thus of the form:*

$$S^e_{11} := \frac{1}{2} \begin{pmatrix} 1 & -1 & 0 \\ -1 & 1 & 0 \\ 0 & 0 & 0 \end{pmatrix}, \quad S^e_{12} := \frac{1}{2} \begin{pmatrix} 1 & 0 & -1 \\ -1 & 0 & 1 \\ 0 & 0 & 0 \end{pmatrix}, \quad S^e_{22} := \frac{1}{2} \begin{pmatrix} 1 & 0 & -1 \\ 0 & 0 & 0 \\ -1 & 0 & 1 \end{pmatrix}. \tag{11}$$

Note that $S^e_{qp} = (S^e_{pq})^T$ holds with $p, q = 1, \ldots, d$ and $d = 2\,(3)$ for triangles (tetrahedra).

Lemma 2.1 *For linear shape functions, the base element matrices for both types of elements can be written in the simplified form*

$$S^e_{pq} = \mid \Omega^{\mathrm{loc}}_e \mid \left[\left(\delta_{i\,(p+1)} - \delta_{i\,1} \right) \left(\delta_{j\,(q+1)} - \delta_{j\,1} \right) \right]_{i,j=1,\ldots,n^e_N} \tag{12}$$

with fixed $p, q \in \{1, \ldots, d = 2\,(3)\}$ and $n^e_N = 3$ (4) for the unit triangle (tetrahedron). Thereby, $\mid \Omega^{\mathrm{loc}}_e \mid$ denotes the area (volume) of the respective local finite element, which is equal to $1/2$ $(1/6)$ for the unit triangle (tetrahedron).

Proof. Due to the simple structure of the derivatives of the shape function for the linear triangle and tetrahedron, as given by Eqs. (9) and (10), respectively, the integrand in Eq. (6) can be expressed as $\Phi_{i,p}(\boldsymbol{\xi})\, \Phi_{j,q}(\boldsymbol{\xi}) = \left(\delta_{i\,(p+1)} - \delta_{i\,1} \right) \left(\delta_{j\,(q+1)} - \delta_{j\,1} \right)$ for arbitrary but fixed $i, j \in \{1, \ldots, n^e_N\}$, where δ_{ik} denotes the well-known Kronecker delta. Integrating the Kronecker delta over the finite element in the local system yields $\displaystyle\int_{\Omega^{\mathrm{loc}}_e} \delta_{ik}\, d\boldsymbol{\xi} = \mid \Omega^{\mathrm{loc}}_e \mid \delta_{ik}$. For the volume of the unit triangle and unit tetrahedron one simply obtains $\mid \Omega^{\mathrm{loc}}_e \mid = \int_0^1 \int_0^{1-\xi_1} d\xi_2 d\xi_1 = \frac{1}{2}$ and $\mid \Omega^{\mathrm{loc}}_e \mid = \int_0^1 \int_0^{1-\xi_1} \int_0^{1-\xi_1-\xi_2} d\xi_3 d\xi_2 d\xi_1 = \frac{1}{6}$, respectively, which completes the proof. □

2.3 Efficient computation of edge matrices for FLIM

In order to extend the concept of base element matrices, as outlined in Section 2.2, to base edge matrices as used in FLIM, we need the shape functions along a reference line in the local coordinate system. The vector of linear shape functions corresponding to the unit line with $\xi \in [0,1]$ (obtained in analogy with FEM) reads as

$$\Phi^C(\xi) = \begin{pmatrix} 1-\xi \\ \xi \end{pmatrix} . \tag{13}$$

For an arbitrary triangle or tetrahedron bounded by line segments we now map each of its edges onto this reference line. To keep the FLIM-structure consistent with FEM, for later use, we extend the size of the vector of shape functions to be again equal to the number of nodes in the finite element. Therefore, we set the linear shape functions at the nodes along a given edge (say at m and n) according to (13) to $1-\xi$ and ξ, while for the remaining nodes in the finite element we simply use zero entries. This is summarized in the following remark.

Remark 2.3 *The vector of shape functions restricted to an edge of unit length between two fixed nodes $m, n \in \{1, \ldots, n_N^e\}$ in a finite element is written as*

$$\Phi_{mn}^{C,e}(\xi) = (1-\xi)\,\mathbf{e}_m + \xi\,\mathbf{e}_n\,, \tag{14}$$

with its derivative w.r.t. ξ given as

$$\Phi_{mn,\xi}^{C,e}(\xi) = -\mathbf{e}_m + \mathbf{e}_n\,. \tag{15}$$

Thereby, $\mathbf{e}_k$ denotes the k-th unit column-vector of dimension n_N^e. That means, for the edge between nodes 1 and 2 in a triangular element, $\Phi_{12}^C := (1-\xi,\, \xi,\, 0)^T$, while for the edge between nodes 4 and 1 in a tetrahedral element, one obtains $\Phi_{41}^C := (\xi,\, 0,\, 0,\, 1-\xi)^T$, where the nodes in the finite element are numbered counter-clockwise.

The unknown function u along an edge can then be expressed via the shape functions, defined in terms of local coordinates, and the corresponding nodal values $u^{(i)}$ with $i = 1, \ldots, n_N^e$ in the whole finite element as $u(\xi) = \Phi_i^{C,e}(\xi)\, u^{(i)}$. In analogy with the base matrices at elemental level we will now set up base matrices at edge level (for each element edge):

Definition 2.2 *The base matrix along an element edge between two fixed nodes m, n in the set $\{1, \ldots, n_N^e\}$ is defined as*

$$S_{mn}^{C,e} := \left(\int_C (\Phi_{mn}^{C,e})_{i,\xi}(\xi)\, (\Phi_{mn}^{C,e})_{j,\xi}(\xi)\, d\xi \right)_{ij} \qquad (i,j = 1, \ldots, n_N^e)\,. \tag{16}$$

Remark 2.4 *By utilizing the derivatives of the shape functions, as given by (15), the (symmetric) base edge matrix corresponding to an edge of unit length between fixed nodes m and n of a finite element ($m, n = 1, \ldots, n_N^e$) can then be written in the form*

$$S_{mn}^{C,e} = \left[(-\delta_{mi} + \delta_{ni})(-\delta_{mj} + \delta_{nj})\right]_{i,j=1,\ldots,n_N^e} \;=\; E_{mm} - E_{mn} - E_{nm} + E_{nn}\,, \tag{17}$$

where δ_{ij} again denotes the well-known Kronecker delta, while E_{ij} designates an $n_N^e \times n_N^e$ matrix with its only non-zero entry at (i, j) being equal to unity.

Using the same partition of $\bar{\Omega}$ into a number of finite elements as in FEM, Eq. (3) also forms the basis for our approximations with FLIM. Again w assume that $c(\mathbf{x}) \equiv 1$, i.e., the identity. Then, instead of computing the integral over a given finite element via Formula (7), the finite line integration method is based on the computation via edge integrals, which yields

$$\int_{\Omega_e} \nabla_k u(\mathbf{x})\, \nabla_k w(\mathbf{x})\, d\mathbf{x} \;=\; \sum_{1 \le m,n \le n_N^e} \bar{\mathbf{w}}\, a_{mn}^C\, S_{mn}^{C,e}\, \bar{\mathbf{u}} \tag{18}$$

with corresponding nodal and coefficient vectors $\bar{\mathbf{u}}$ and $\bar{\mathbf{w}}$ and multiplication factors a_{mn}^C, which are yet to be determined.

To ensure similar convergence properties for the edge approach compared to the finite element method, in general, one has to determine the multiplication factors a_{mn}^C for the base edge matrices such that the resulting matrices at element level, obtained from either the element or the edge approach, are at least spectrally equivalent[1]. For triangular and tetrahedral elements bounded by line segments, however, it can even be shown that for properly chosen factors for the base edge matrices, the resulting element stiffness matrix obtained by assembling the base matrices at edge level in FLIM can always be made identical to its FEM-counterpart. Note that the resulting global stiffness matrices will then also be identical. The computation of the multiplication factors in FLIM with this special property is subject of the following statement:

Theorem 2.1 *Let a_{pq}, S_{pq}^e and $S_{mn}^{C,e}$ be as defined in Defs. 2.1 and 2.2. To ensure identical element stiffness matrices for FEM and FLIM, the factors for the base edge matrices must satisfy the following relation obtained from equating Formulae* (7) *and* (18)*:*

$$\sum_{1 \le p,q \le d} a_{pq}\, S_{pq}^e \;=\; \sum_{1 \le m < n \le n_N^e} a_{mn}^C\, S_{mn}^{C,e}\,. \tag{19}$$

For the triangle the factors are given by

$$a_{mn}^C = \frac{1}{2\,J}\, \langle\, \mathbf{x}^{m-j},\; \mathbf{x}^{n-j} \,\rangle \tag{20}$$

with $j \in \{1, \ldots, n_N^e\} \backslash \{m, n\}$ fixed and $J := (x_{21} - x_{11})(x_{32} - x_{12}) - (x_{31} - x_{11})(x_{22} - x_{12})$, where $x_{ik} := x_k^i$ denotes the k-th component of node x^i, while for the tetrahedron one obtains

$$a_{mn}^C = \frac{1}{6\,J}\, \langle\, \mathbf{x}^{i-j} \wedge \mathbf{x}^{m-j},\; \mathbf{x}^{i-j} \wedge \mathbf{x}^{n-j} \,\rangle \tag{21}$$

with $i > j \in \{1, \ldots, n_N^e\} \backslash \{m, n\}$ fixed. The scalar and vector product of two vectors $\mathbf{a}$ and $\mathbf{b}$ are respectively denoted as $\langle \mathbf{a}, \mathbf{b} \rangle$ and $\mathbf{a} \wedge \mathbf{b}$. The Jacobian for the linear mapping is given by $J := \det \frac{\partial \mathbf{x}(\xi)}{\partial \xi} = \varepsilon_{ijk}\; \mathbf{x}_i^{2-1}\; \mathbf{x}_j^{3-1}\; \mathbf{x}_k^{4-1}$ (summation over i, j, k), where $\mathbf{x}_k^{i-j} := x_k^i - x_k^j$ and ε_{ijk} designates the ε-permutation tensor, which is 1 (-1) for even (odd) permutations of $(1, 2, 3)$, and zero otherwise (see (22) *below).*

[1] Two $m \times m$ matrices $\mathbf{A}$ and $\mathbf{B}$ are said to be *spectrally equivalent*, if there exist positive constants c_1 and c_2 such that $c_1 \le \mid \lambda_i \mid \le c_2$ for all $i = 1, \ldots, m$, where λ_i denotes the i-th eigenvalue of the matrix $\mathbf{B^{-1}A}$.

Proof. Since the resulting stiffness matrix at elemental level is symmetric, we obtain the following six equations by utilizing Eqs. (8), (11) and (17) in Eq. (19), by multiplying them with -1, and by reordering:

$$\begin{aligned}
-(a_{12}^C + a_{13}^C) &= -\frac{1}{2}(a_{11} + 2a_{12} + a_{22}) & -(a_{12}^C + a_{23}^C) &= -\frac{1}{2}a_{11} \\
-(a_{13}^C + a_{23}^C) &= -\frac{1}{2}a_{22} & a_{12}^C &= +\frac{1}{2}(a_{11} + a_{12}) \\
a_{13}^C &= +\frac{1}{2}(a_{12} + a_{22}) & a_{23}^C &= -\frac{1}{2}a_{12}\,.
\end{aligned}$$

The factors a_{12}^C, a_{13}^C, and a_{23}^C can now directly be obtained from the last three equations and it can be shown easily that they also satisfy the remaining equations. Making use of Eq. (8) and of the fact that

$$\mathbf{x}^{i-j} + \mathbf{x}^{j-k} := \mathbf{x}^i - \mathbf{x}^j + \mathbf{x}^j - \mathbf{x}^k = \mathbf{x}^{i-k}$$

for arbitrarily chosen $i, j, k \in \{1, \ldots, n_N^e\}$, and by reordering the terms appropriately, Formula (20) is obtained.

With the base element matrices for the tetrahedron obtained from Eq. (10), by utilizing Eqs. (8) and (17) and by using the fact that the resulting stiffness matrix at elemental level is again symmetric, the factors for the base edge matrices are now obtained from the following ten equations, derived from Eq. (19):

$$\begin{aligned}
-(a_{12}^C + a_{13}^C + a_{14}^C) &= -\frac{1}{6}\sum_{1\le i,j\le 3} a_{ij} & -(a_{12}^C + a_{23}^C + a_{24}^C) &= -\frac{1}{6}a_{11} \\
-(a_{13}^C + a_{23}^C + a_{34}^C) &= -\frac{1}{6}a_{22} & -(a_{14}^C + a_{24}^C + a_{34}^C) &= -\frac{1}{6}a_{33} \\
a_{12}^C &= +\frac{1}{6}(a_{11} + a_{12} + a_{13}) & a_{13}^C &= +\frac{1}{6}(a_{12} + a_{22} + a_{23}) \\
a_{14}^C &= +\frac{1}{6}(a_{13} + a_{23} + a_{33}) & a_{23}^C &= -\frac{1}{6}a_{12} \\
a_{24}^C &= -\frac{1}{6}a_{13} & a_{34}^C &= -\frac{1}{6}a_{23}\,.
\end{aligned}$$

The equations above were ordered such that the factors a_{mn}^C with $1 \le m < n \le 4$ can directly be obtained from the last six equations. These factors are, thereby, given in dependence on the a_{pq}-factors (see Eq. (5)) for the base element matrices. By utilizing the ε-permutation tensor, defined as

$$\varepsilon_{ijk} := \begin{cases} 1, & \text{if } (i,j,k) \text{ is an even permuation of } (1,2,3) \\ -1, & \text{if } (i,j,k) \text{ is an odd permuation of } (1,2,3) \\ 0, & \text{otherwise}\,, \end{cases} \tag{22}$$

we can write (by summing over i and j)

$$J\,\xi_{p,k} = \varepsilon_{ijk}\, x_i^{m(p)-1}\, x_j^{n(p)-1}, \tag{23}$$

where $(m(p), n(p))$ are given as the entries at position $(p+1, p+2)$ of the sequence $2, 3, 4, 2, 3$. The factors a_{pq} with $p, q = 1, \ldots, d\,(= 3)$ can thus be rewritten as

$$\begin{aligned} a_{pq} &= J\,\xi_{p,k}\,\xi_{q,k} \\ &= \frac{1}{J}\,\varepsilon_{ijk}\,x_i^{m(p)-1}\,x_j^{n(p)-1}\,\varepsilon_{rsk}\,x_r^{m(q)-1}\,x_s^{n(q)-1} \\ &= \frac{1}{J}\,\langle \mathbf{x}^{m(p)-1} \wedge \mathbf{x}^{n(p)-1},\ \mathbf{x}^{m(q)-1} \wedge \mathbf{x}^{n(q)-1} \rangle\,, \end{aligned} \tag{24}$$

where $\mathbf{a} \wedge \mathbf{b}$ denotes the vector product of $\mathbf{a}$ and $\mathbf{b}$.

For a_{23}^C, a_{24}^C, and a_{34}^C we immediately obtain the expressions in Formula (21) by inserting Eq. (24) and using the corresponding settings for $m(.)$ and $n(.)$ in their definitions above. For a_{12}^C the derivation of Formula (21) is as follows:

$$\begin{aligned} a_{12}^C &= \frac{1}{6}\sum_{k=1}^{3} a_{1k} \overset{(24)}{=} \frac{1}{6J}\,\langle\, \mathbf{x}^{m(1)-1} \wedge \mathbf{x}^{n(1)-1},\ \sum_{k=1}^{3} \left(\mathbf{x}^{m(k)-1} \wedge \mathbf{x}^{n(k)-1}\right) \rangle \\ &= \frac{1}{6J}\,\langle \mathbf{x}^{3-1} \wedge \mathbf{x}^{4-1},\ \mathbf{x}^{3-1} \wedge \mathbf{x}^{4-1} + \mathbf{x}^{4-1} \wedge \mathbf{x}^{2-1} + \mathbf{x}^{2-1} \wedge \mathbf{x}^{3-1} \rangle \\ &= \frac{1}{6J}\,\langle \mathbf{x}^{3-1} \wedge \mathbf{x}^{4-1},\ \mathbf{x}^{4-1} \wedge \mathbf{x}^{2-3} + \mathbf{x}^{2-1} \wedge \mathbf{x}^{3-2} \rangle \\ &= \frac{1}{6J}\,\langle \mathbf{x}^{4-3} \wedge \mathbf{x}^{1-3},\ \mathbf{x}^{4-3} \wedge \mathbf{x}^{2-3} \rangle\,, \end{aligned} \tag{25}$$

where we used the fact that $\mathbf{x}^{i-j} + \mathbf{x}^{j-k} = \mathbf{x}^{i-k}$ and that $\langle \mathbf{x}^{i-j} \wedge \mathbf{x}^{k-j} \rangle = \langle \mathbf{x}^{i-j} \wedge \mathbf{x}^{k-i} \rangle$ since $\langle \mathbf{x}^{i-j} \wedge \mathbf{x}^{i-j} \rangle = 0$ for arbitrary $i, j, k \in \{1, \ldots, n_N^e\}$, chosen appropriately. The correctness of Formula (21) for the remaining factors a_{13}^C and a_{14}^C can be shown analogously. This completes the proof. □

Remark 2.5 *The factors a_{mn}^C for linear triangular elements can be calculated as the scalar product of the two vectors formed by the edge nodes with the opposing corner node in the triangle and by dividing this product by four times the area of the triangle (see Fig. 1). This is equivalent to calculating the scalar product of the normals onto the edge-opposing vectors and dividing by $2J$.*

Each factor for the tetrahedron is simply the scalar product of the two normal vectors onto the areas, which share only one node with the edge under consideration. One normal vector, thereby, points into the tetrahedron, whereas the second normal vector points outwards, as illustrated in Fig. 1.

Note that the scaling factors, $1/2$ for the triangle and $1/6$ for the tetrahedron, are exactly equal to the ratio of the L_2-product of the shape function derivatives evaluated for the reference (unit) element and edge in the local coordinate system, respectively. These scaling factors are also equal to the area and volume of the corresponding reference element (cf. Lemma 2.1).

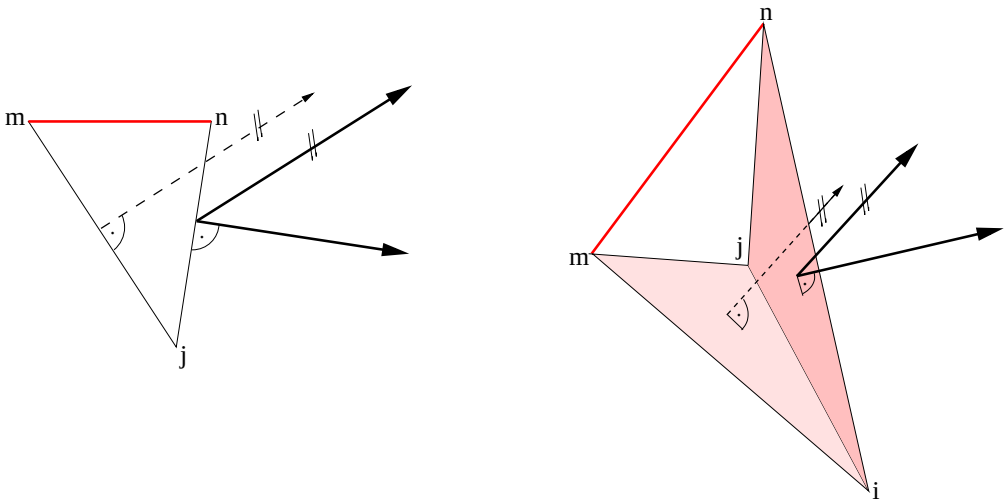

Figure 1: Illustration of the computation of an a^C_{mn} in a triangle and in a tetrahedron.

2.4 Computation of edge load vectors

Since the element stiffness matrices, either obtained directly (FEM) or via assemblage of base edge matrices (FLIM), are identical for triangular and tetrahedral elements, the load vector for FLIM - obtained via integration along edges - is now to be determined such that it reflects the FEM load. In particular, this means that the solution based on the FLIM load should result in an approximation error of the same order as compared to FEM.

Let us consider the load in a specific node p. The total load in this node p is obtained, according to FEM, as the sum of loads calculated over all elements which enter in node p (denoted by $e(p)$), i.e.

$$\ell^e(p) = \sum_{e(p)} \int_{\Omega_e^{loc}} f(\xi)\, \Phi_i(\xi)\, \overline{w}^{(i)}\, J(\xi)\, d\xi\,, \tag{26}$$

For FLIM, however, the total load is the sum of all loads calculated along all edges, which are linked with node p (let $C(p)$ denote the total number of such edges), and may thus be written as

$$\ell^C(p) = \alpha(p) \sum_{C(p)} \int_{C_n} f(t)\, \left(\Phi^C_{p-n}\right)_k (t)\, \overline{w}^{(k)}\, dt\,. \tag{27}$$

The scaling factor $\alpha(p)$ now has to be determined such as to ensure that both loads agree in the limit. A suitable choice is therefore given by

$$\alpha(p) = \frac{2}{n_N!}\, \frac{\sum_{e(p)} \bar{f}_e\, J_e}{\sum_{c(p)} \bar{f}_c\, l_c}\,, \tag{28}$$

where J_e (which is constant in the case of linear elements) denotes the Jacobian of the transformation to the reference element (which is twice the area of the specific element in two dimensions), l_c is the length of edge $c(p)$, and $\bar{f}_e$ and $\bar{f}_c$ designate the intermediate

value of f according to the Mean Value Theorem for Integration at element and edge level, respectively. Note that for constant right-hand sides f the setting for $\alpha(p)$ simplifies to

$$\alpha(p) = \frac{2}{n_N!} \frac{\sum_{e(p)} J_e}{\sum_{c(p)} l_c}, \tag{29}$$

which ensures that the FEM-load and thus an identical solution compared to FEM is obtained. In general, however, the FLIM solution will deviate from the FEM solution.

3 Approximation and consistency error estimates for FLIM as compared to FEM

According to Theorem 2.1, the element stiffness matrices and, consequently, the global stiffness matrices obtained by FLIM and FEM are identical. The approximations of the linear functionals, however, are different in general. In the case of finite line integration, the load is calculated along the edges of a given finite element, while in FEM the load is computed by integrating over the finite element itself. In order to maintain the approximation and consistency properties of the finite element method also for FLIM, we thus have to ensure that the right-hand sides are approximated to the same degree of accuracy.

3.1 Summary of the theory for FEM as required for FLIM

In the sequel we consider a family of finite element spaces X_h made up of finite elements (K, P_K, Σ_K), where $K \in \mathcal{T}_h$ is a finite element of the triangulation $\mathcal{T}_h$ of the set $\bar{\Omega}$, the space $P_K := \{v_h|_K : v_h \in X_h\}$ denotes a (finite-dimensional) space of functions $v_h \in X_h$ restricted to K, and Σ_K designates the set of degrees of freedom of a finite element. If $P_K \subset H^1(K)$ - where henceforth we shall write $H^1(K)$ instead of $H^1(\overset{\circ}{K})$ - is satisfied for all $K \in \mathcal{T}_h$ and $X_h \subset \mathcal{C}^0(\bar{\Omega})$, where $\mathcal{C}^m(A)$ denotes the space of m-times continuously differentiable functions on a subset $A \subset \mathbb{R}^n$, then the inclusions $X_h \subset H^1(\Omega)$ and $X_{oh} := \{v_h \in X_h : v_h = 0 \text{ on } \Gamma_D\} \subset H_0^1(\Omega)$ hold (cf. Ciarlet [3]). Thereby, $H_0^1(\Omega) := \{v \in H^1(\Omega) : v = 0 \text{ on } \Gamma_D\}$ and Γ_D denotes the Dirichlet boundary.

Throughout this section, we make the following standard assumptions (cf. Ciarlet [3]):

(H1) The associated family of triangulations $\mathcal{T}_h$ is regular.

(H2) All the finite elements (K, P_K, Σ_K), $K \in \bigcup_h \mathcal{T}_h$, are affine-equivalent to a single reference element $(\hat{K}, \hat{P}, \hat{\Sigma})$.

(H3) All the finite elements (K, P_K, Σ_K), $K \in \bigcup_h \mathcal{T}_h$, are of class $\mathcal{C}^0$.

Let us assume that the domain $\bar{\Omega}$ is polygonal. Then, the set $\bar{\Omega}$ can be exactly covered by triangulations based on linear triangles and the inclusion $V_h \subset V$ still holds, where $V = H_0^1(\Omega)$ and $V_h := \{v_h \in X_h : v_h = 0 \text{ on } \Gamma_D\}$. As a consequence of (H1) to (H3), the

inclusions $X_h \subset H^1(\Omega)$ and $V_h \subset H^1_0(\Omega)$ are satisfied as long as the inclusion $\hat{P} \subset H^1(\hat{K})$ (which we shall assume) holds. In practice, the integrals which appear in the bilinear form and the linear functional are almost always approximated by numerical integration. The corresponding discrete problem can thus be written in the form:

Given a space V_h, find a discrete solution $u_h \in V_h$ such that

$$a_h(u_h, v_h) \;=\; f_h(v_h), \quad \forall\, v_h \in V_h, \tag{30}$$

where, for all functions u_h, $v_h \in V_h$, the approximate bilinear form $a_h(.,.)$ and the approximate linear form $f_h(.)$ are given by

$$a_h(u_h, v_h) \;:=\; \sum_{K \in \mathcal{T}_h} \sum_{l=1}^{L} \omega_l^K \sum_{i,j=1}^{n} \left(a_{ij}\, u_{h,i}\, v_{h,j}\right)(b_l^K)\,, \tag{31}$$

$$f_h(v_h) \;:=\; \sum_{K \in \mathcal{T}_h} \sum_{l=1}^{L} \omega_l^K \left(f\, v_h\right)(b_l^K)\,. \tag{32}$$

Thereby, ω_l^K denotes a weight and the point b_l^K designates a node in the quadrature formula $\int_K \varphi(x)dx \;\approx\; \sum_{l=1}^{L} \omega_l^K\, \varphi(b_l^K)$. The numerical integration, thereby, is performed over the reference element $\bar{K}$ rather than over the finite element K, which are related by an invertible affine mapping

$$F_K :\, \hat{K} \to K \quad \text{with} \quad F_K(\xi) := B_K\, \xi + b_K\,,$$

which maps $\hat{K}$ onto K. Assuming, without loss of generality, that the (constant) Jacobian of the mapping F_K, $J := \det B_K$, is positive, one can write

$$\int_K \varphi\,(x)\, dx = J \int_{\hat{K}} \hat{\varphi}\,(\xi)\, d\xi\,, \tag{33}$$

where the functions $\varphi(x)$ and $\hat{\varphi}$ are related according to $\varphi(x) = \hat{\varphi}(\xi)$ for all $x = F_K(\xi)$ with $\xi \in \hat{K}$. Using a quadrature scheme for the numerical integration over the set $\hat{K}$ consists in an approximation via a finite sum of the form

$$\int_{\hat{K}} \hat{\varphi}(\xi)\, d\xi \approx \sum_{l=1}^{L} \hat{\omega}_l\, \hat{\varphi}\,(\hat{b}_l), \tag{34}$$

where the weights and nodes in the quadrature formulae over the sets K and $\hat{K}$ are defined as $\omega_l^K = J\,\hat{\omega}_l$ and $b_l^K = F_K(\hat{b}_l)$, respectively. Consequently only a numerical quadrature scheme over the reference finite element needs to be considered.

Let the norm of the space V be denoted by $\|.\|$ and let us assume that the functions $a_{ij} \in L^\infty(\Omega)$ and $f \in L^2(\Omega)$ are defined everywhere over $\bar{\Omega}$. The first lemma of Strang then provides an error estimate for discrete problems with approximated bilinear forms and approximated linear functionals, which states:

Theorem 3.1 *(First Strang lemma). Consider a family of discrete problems for which the associated approximate bilinear forms are uniformly V_h-elliptic.*

Then there exists a constant C independently of the space V_h such that

$$\|u - u_h\| \leq C \left(\inf_{v_h \in V_h} \left[\|u - v_h\| + \sup_{w_h \in V_h} \frac{|a(v_h, w_h) - a_h(v_h, w_h)|}{\|w_h\|} \right] + \sup_{w_h \in V_h} \frac{|f(w_h) - f_h(w_h)|}{\|w_h\|} \right). \tag{35}$$

A proof of this theorem can be found in Ciarlet [3]. In this reference it is also shown that under certain conditions on the quadrature scheme it can be ensured that the approximate bilinear form is uniformly V_h-elliptic and that the order of convergence, obtained in the absence of numerical integration, then remains unaltered by the effect of quadrature: Restricting, for simplicity, to the case where $P_K = P_k(K)$ for all finite elements $K \in \mathfrak{T}_h$, where $P_k(K)$ denotes the space of all polynomials over the finite element K of degree $\leq k$ for some integer $k \geq 1$, the main result briefly states that one has

$$\|u - u_h\|_{1,\Omega} = \mathcal{O}(h^k)$$

provided the quadrature formula is exact for all polynomials of degree $2k - 2$. The proof of this latter result depends on the Bramble-Hilbert lemma (cf. Theorem 4.1.3 in Ciarlet [3]).

3.2 Construction of proper quadrature schemes for FLIM

Replacing the integral over a given finite element by integrals over its edges, does not alter the bilinear form in the discrete problem (30), as given by (31), if the multiplication factors for FLIM are computed according to Theorem 2.1. Since the vector space V_h^C for FLIM contains all functions of V_h restricted to the union of the edges of all finite elements (edge skeleton), we have $V_h|_C \subset V_h^C$. On the other hand, if we assume that every element in V_h^C is a function of V_h (restricted to the edges), i.e., $V_h^C \subset V_h$. Consequently, we have $V_h^C \equiv V_h$ and can therefore apply the first lemma of Strang directly to FLIM, which thus allows the computation of the approximation error $\|u - u_h\|$ in the same way as done for FEM.

Let us assume that we already use a quadrature scheme in the finite element method, which ensures that the order of convergence is maintained in the case of numerical integration, as required from theory. In view of Theorem 2.1 and for sufficiently regular u (see below) we conclude: To obtain the same order of convergence for FLIM it is sufficient to ensure that the quadrature rule used is of the same order of accuracy as its FEM-counterpart. Moreover, if there exists a quadrature scheme for FLIM and FEM which provides identical approximations of the linear functional, we are done. The derivation of such quadrature schemes will be dealt with next.

First, let us note that for linear finite elements it can be shown (cf. Ciarlet [3]) that

$$\|u - u_h\|_{0,2,\Omega} = \mathcal{O}(h^2) \tag{36}$$

measures the error in the L^2-norm over Ω provided that u satisfies a regularity condition, viz., $u \in H^2(\Omega)$, and the quadrature scheme is at least exact for constant functions. For linear finite elements in two and three dimensions this can already be achieved by utilizing quadrature rules based on barycentric coordinates in the corresponding n-simplex. Such

quadrature schemes, however, are not suitable for FLIM since we need the integration points to be located on the edges. In the following we thus seek quadrature schemes, where the integration points are located along the edges, and try to adapt the weights in such a way that these schemes are equally suited for computations with FEM and FLIM:

In two dimensions, we solve the equation

$$\sum_{i=1}^{3} p(\hat{m}_i)\, \hat{\omega}_i\, J \;=\; \sum_{k=1}^{3} \ell_k\, p(\hat{m}_k)\, \hat{\tilde{\omega}}_k^c\,, \tag{37}$$

where J designates the Jacobian for the transformation from global to local coordinates, as defined prior to Eq. (33), ℓ_k is the length of the edge and $\hat{m}$ denotes the midpoint at an edge of the reference finite element. The weights $\hat{\omega}_k^c$ corresponding to the quadrature formula used for the integration along the reference (unit) line c are then obtained from their counterparts $\hat{\omega}_i$ for the quadrature formula for the reference finite element $\hat{K}$ as follows:

$$\hat{\tilde{\omega}}_j^c = \frac{J\,\hat{\omega}_j}{3\ell_j} \qquad \text{with} \qquad \hat{\omega}_j = \frac{1}{3} \qquad \forall\, j = 1,2,3\,. \tag{38}$$

Note that the quadrature formula on the left-hand side is exact for polynomials $p \in P_2(\hat{K})$ in the triangle $\hat{K}$, i.e.,

$$\forall\, p \in P_2(\hat{K}) : \; \int_{\hat{K}} p\,(\xi)\, d\xi - \frac{J}{3} \sum_{i=1}^{3} p(\hat{m}_i) = 0.$$

In three dimensions, we seek a quadrature formula for the reference tetrahedron where the integration points are either corner nodes c_{kj} or midpoints m_k at the k-th edge with length ℓ_k and $k = 1, \ldots, 6$. The set $\{a_1, \ldots, a_{10}\}$ is defined as the union of corner nodes and midpoints along the edges of the tetrahedron. Hence, we equate

$$\sum_{i=1}^{10} p(a_i)\, \hat{\omega}_i^a\, J \;=\; \sum_{k=1}^{6} \ell_k \left(p(m_k)\, \hat{\tilde{\omega}}_k^m + \sum_{j=1}^{2} p(c_{kj})\, \hat{\tilde{\omega}}_j^c \right), \tag{39}$$

where $\hat{\tilde{\omega}}^m$ and $\hat{\tilde{\omega}}^c$ are respectively the weights at the midpoints and corner nodes in the quadrature formula for the integration along edges. From Equation (39) we thus obtain

$$\hat{\tilde{\omega}}_i^m = \frac{J\,\hat{\omega}_i^m}{\ell_i} \quad \text{with} \quad \hat{\omega}_i^m = \frac{1}{5} \qquad \text{and} \qquad \hat{\tilde{\omega}}_j^c = \frac{J\,\hat{\omega}_j^c}{\ell_j} \quad \text{with} \quad \hat{\omega}_j^c = -\frac{1}{20}\,, \tag{40}$$

where $i = 1(1)6$ and $j = 1(1)4$. The weights at the six midpoints along the edges and at the four vertices (corner nodes) of the tetrahedron are denoted by $\hat{\omega}_i^m$ and $\hat{\omega}_i^c$, respectively. Note that the quadrature scheme on the left-hand side of (39) is exact for polynomials $p \in \mathbf{P}_2(\hat{K})$ in the reference tetrahedron $\hat{K}$.

Under the assumption of sufficient regularity of u, the quadrature schemes derived above in two and three dimensions can now equally be used in FEM- and FLIM-computations. Furthermore, these quadrature schemes ensure that the error estimate (36) is valid for both methods.

Remark 3.1 *(Subparametric elements): Note that Eq.* (33) *is not restricted to linear isoparametric elements, but equally holds for subparametric elements, where more nodes are used to define u than to define the geometry and where a linear mapping is utilized between the global and local coordinate system. Based on the quadrature schemes, derived above, this extension to include subparametric elements can then also be applied to the finite line integration method.*

Remark 3.2 *(Storage): In Table 1 the storage requirement (number of entries) for element matrices (ElMat) and edge matrices (EdMat) to be used for the assemblage of the global stiffness matrix is summarized for 2D- and 3D- scalar problems and systems of partial differential equations. The quantities presented are normalized with respect to the number of elements* n_e*. Thereby, the number of edges is assumed to be approximately equal to* $2\,n_e$ *in 2D and to* $3\,n_e$ *in 3D, which is true for sufficiently large problems.*

Scalar problems	ElMat	EdMat	Saving factor for FLIM (in %)
2D	6	2	66.7
3D	10	3	70.0
Vector problems			
2D	21	4	80.9
3D	78	9	91.0

Table 1: Comparison of the storage requirement.

The overall saving of FLIM over the element-based FEM amounts to about 67 per cent in the 2D-case and goes up to even 90 per cent in three dimensions. Further, there is no overhead for storing the edge matrices as compared to the storage required for the global stiffness matrix in FLIM, while the overhead for utilizing element matrices in FEM amounts to 200% in 2D and even up to 900% for 3D vector problems.

Thereby, we assume that the edge and element matrices are stored. This assumption is well-founded since it is known that the information contained in these matrices is vital for the development of efficient and problem-adapted linear solvers (cf. Remark 3.3).

Note that the (constant) Jacobian J and of the lengths of the edges (finite lines) l_c *can be computed a-priori in FLIM, which reduces the computational effort.*

Remark 3.3 *(AMG - Algebraic multigrid): Based on the knowledge of edge matrices, the concept of strong and weak connections, as used in classical AMG (cf. Ruge and Stüben [9]), can now be generalized to non-M matrices. This approach allows for the construction of efficient coarsening and interpolation schemes in a so-called molecule-based AMG (AMGm), as shown by Kraus et al. [6] and [7].*

4 Numerical Convergence Results - FLIM versus FEM

In this section the new method based on line integration, termed FLIM, is applied to three different problems with the right-hand side f ranging from a constant to a highly nonlinear function. Since the numerical tests were performed using the Partial Differential Equation Toolbox of the commercial finite element software package Matlab of The MathWorks and the Matlab environment itself, the test problems were set up in two dimensions. However, with a proper quadrature rule, as outlined in the previous section, the same performance can be ensured for FLIM when applied to problems in three dimensions. For each case the numerical solution obtained via the finite line integration method is compared with its FEM-counterpart obtained with Matlab. The Gaussian quadrature used for the numerical integration in FEM in Matlab is based on the Gaussian points, which do not lie on the edges. Consequently, the approximation errors of FEM and FLIM are expected to be different, but of the same order. The error in the following examples is measured in both the L^∞- and the L^2-norm, which are denoted by $\|.\|_\infty$ and $\|.\|_2$, respectively.

The problems considered herein are of the form:

$$\begin{aligned} -\mathrm{div}\,[\,\mathrm{grad}\,u(\mathbf{x})] &= f(\mathbf{x}) \qquad \text{in} \quad \Omega\,(\subset \mathbb{R}^2) \\ u(\mathbf{x}) &= 0 \qquad\quad \text{on} \quad \Gamma_D := \partial\Omega\,, \end{aligned} \tag{41}$$

where the right-hand side, the exact solution, and the domain Ω are specified for each case in Table 2.

Case	$f(\mathbf{x})$	$u_{\mathrm{ex}}(\mathbf{x})$	Ω
1	-4	$x_1^2 + x_2^2$	$[0,2]^2$
2	$-2\,x_2$	$x_1^2\,x_2$	$[0,2]^2$
3	$-4\,(x_1^2 + x_2^2)\,e^{x_1^2 - x_2^2}$	$e^{x_1^2 - x_2^2}$	$[0,1]^2$

Table 2: Details on the three test cases considered.

As can be seen from the results, as presented in Tables 3 to 5 for the three test cases and for different mesh size (as indicated by the number of finite elements n_e), the finite line integration method performs as good as the finite element method, with the same order of the approximation error and convergence rate as FEM. Measured in the L^2-norm, the convergence of FLIM is indeed of the order $\mathcal{O}(h^2)$, which (numerically) verifies our theoretical results stated in the previous section.

For constant right-hand sides the numerical results obtained with FLIM and FEM are identical for uniform (structured) and for unstructured meshes, as depicted in Tables 3. For linear right-hand sides, this coincidence holds only in the case of uniformly structured meshes,

Constant f - FLIM versus FEM				
n_e	$\|u_{\text{FLIM}} - u_{\text{ex}}\|_\infty$	$\|u_{\text{FLIM}} - u_{\text{ex}}\|_2$	$\|u_{\text{FEM}} - u_{\text{ex}}\|_\infty$	$\|u_{\text{FEM}} - u_{\text{ex}}\|_2$
Uniform triangles:				
256	1.042e-2	6.920e-3	1.042e-2	6.920e-3
1024	2.604e-3	1.785e-3	2.604e-3	1.785e-3
4096	6.510e-4	4.532e-4	6.510e-4	4.532e-4
16384	1.628e-4	1.142e-4	1.628e-4	1.142e-4
Unstructured mesh:				
312	6.978e-3	2.810e-3	6.978e-3	2.810e-3
1248	2.452e-3	6.601e-4	2.452e-3	6.601e-4
4992	8.160e-4	1.607e-4	8.160e-4	1.607e-4
19968	2.523e-4	3.986e-5	2.523e-4	3.986e-5
79872	7.494e-5	9.955e-6	7.494e-5	9.955e-6

Table 3: Approximation errors for Case 1.

as can be seen from the results in Table 4. These observations are in agreement with the theory derived in the previous section. The numerical results, as depicted in Table 5 for a nonlinear right-hand side f, confirm the suitability of the quadrature scheme, as derived in Section 3 for the finite line integration method, and show that FLIM is a true, but far less time-consuming alternative to the element-based approach. It again should be emphasized that the approximation errors would be identical in all cases if the FEM-solution was computed with the quadrature schemes given by Eqs. (37) to (40) rather than using the routines of the software package Matlab.

5 Concluding Remarks

A new variant of finite element modelling and of solving partial differential equations based on integration along finite lines (edges) rather than over finite elements was proposed. It was shown that for linear finite elements and properly chosen quadrature schemes the finite line integration method (briefly, FLIM) exhibits the same approximation error and convergence property as the finite element method based on element integration, but results in a faster setup and requires much lower storage than FEM. The new approach allows for a direct computation of the edge matrices and no overhead is produced when storing the edge matrices compared to the storage required for the global stiffness matrix. The information contained in the edge matrices can advantageously be used to construct efficient coarsening and interpolation schemes in algebraic multigrid methods, which can be exploited in the development of improved and problem-adapted linear solvers.

Linear f - FLIM versus FEM				
n_e	$\|u_{\text{FLIM}} - u_{\text{ex}}\|_\infty$	$\|u_{\text{FLIM}} - u_{\text{ex}}\|_2$	$\|u_{\text{FEM}} - u_{\text{ex}}\|_\infty$	$\|u_{\text{FEM}} - u_{\text{ex}}\|_2$
Uniform triangles:				
256	9.766e-3	3.988e-3	9.766e-3	3.988e-3
1024	2.523e-3	1.030e-3	2.523e-3	1.030e-3
4096	6.409e-4	2.616e-4	6.409e-4	2.616e-4
16384	1.615e-4	6.593e-5	1.615e-4	6.593e-5
Unstructured mesh:				
312	7.325e-3	2.264e-3	7.176e-3	2.267e-3
1248	2.401e-3	5.303e-4	2.398e-3	5.315e-4
4992	8.093e-4	1.291e-4	8.237e-4	1.295e-4
19968	2.578e-4	3.205e-5	2.611e-4	3.215e-5
79872	7.820e-5	8.006e-6	7.901e-5	8.031e-6
319488	2.298e-5	2.003e-6	2.318e-5	2.009e-6

Table 4: Approximation errors for Case 2.

Nonlinear f - FLIM versus FEM				
n_e	$\|u_{\text{FLIM}} - u_{\text{ex}}\|_\infty$	$\|u_{\text{FLIM}} - u_{\text{ex}}\|_2$	$\|u_{\text{FEM}} - u_{\text{ex}}\|_\infty$	$\|u_{\text{FEM}} - u_{\text{ex}}\|_2$
Uniform triangles:				
256	5.558e-3	1.691e-3	5.314e-3	1.515e-3
1024	1.562e-3	4.420e-4	1.542e-3	3.954e-4
4096	4.153e-4	1.126e-4	4.139e-4	1.007e-4
16384	1.072e-4	2.840e-5	1.071e-4	2.539e-5
Unstructured mesh:				
312	5.861e-3	9.904e-4	5.724e-3	8.310e-4
1248	1.991e-3	2.289e-4	1.960e-3	1.852e-4
4992	6.414e-4	5.538e-5	6.338e-4	4.392e-5
19968	1.975e-4	1.371e-5	1.955e-4	1.079e-5
79872	5.875e-5	3.420e-6	5.824e-5	2.688e-6
319488	1.704e-5	8.550e-7	1.691e-5	6.716e-7

Table 5: Approximation errors for Case 3.

Acknowledgements

The author would like to thank J. Kraus for valuable discussions and his support.

References

[1] D. Braess: Finite Elemente: Theorie, schnelle Löser und Anwendungen in der Elastizitätstheorie, 3rd ed., Berlin: Springer 2003.

[2] S.C. Brenner, L.R. Scott: The Mathematical Theory of Finite Element Methods, Berlin, London, New York: Springer 1994.

[3] P.G. Ciarlet: The Finite Element Method for Elliptic Problems. Philadelphia: SIAM 2002.

[4] W. Hackbusch: On First and Second Order Box Schemes, Computing 41 (1989), 277-296.

[5] C. Johnson: Numerical solution of partial differential equations by the finite element method, Cambridge, New York: Cambridge University Press 1987.

[6] J. Kraus: Algebraic multigrid based on computational molecules, 2: Systems of elliptic partial differential equations, RICAM-Report 2005-19 (2005).

[7] J. Kraus and J. Schicho: Algebraic Multigrid Based on Computational Molecules, 1: Scalar Elliptic Problems, Computing 77 (2006), 57-75.

[8] M. Křížek, P. Neittaanmäki: Finite Element Approximation of Variational Problems and Applications, New York: Longman 1990.

[9] J.W. Ruge and K. Stüben: Efficient solution of finite difference and finite element equations by algebraic multigrid (AMG). In: Multigrid Methods for Integral and Differential Equations, D.J. Paddon and H. Holstein, eds., The Institute of Mathematics and Its Applications Conference Series, Clarendon Press, Oxford, 1985, 169-212.

[10] H.R. Schwarz: Methode der finiten Elemente, 3rd ed., Stuttgart: Teubner 1991.

[11] J. Synka and J. Kraus: FLIM - A Variant of FEM based on Line Integration, PAMM-Proc. Appl. Math. Mech. 5 (2005), 847-848.

[12] O.C. Zienkiewicz, R.L. Taylor: The Finite Element Method, 5th ed., Vol. 1-3, Amsterdam, Boston, London: Butterworth-Heinemann 2000.

[13] O.C. Zienkiewicz, R.L. Taylor, and P. Nithiarasu: The Finite Element Method for Fluid Dynamics, 6th ed., Amsterdam, Boston, London: Elsevier Butterworth-Heinemann 2005.